

Fluid-like behavior of a one-dimensional granular gas

Fabio Cecconi, Fabiana Diotallevi, Umberto Marini Bettolo Marconi, and Andrea Puglisi

Citation: *J. Chem. Phys.* **120**, 35 (2004); doi: 10.1063/1.1630957

View online: <http://dx.doi.org/10.1063/1.1630957>

View Table of Contents: <http://jcp.aip.org/resource/1/JCPSA6/v120/i1>

Published by the [American Institute of Physics](#).

Additional information on *J. Chem. Phys.*

Journal Homepage: <http://jcp.aip.org/>

Journal Information: http://jcp.aip.org/about/about_the_journal

Top downloads: http://jcp.aip.org/features/most_downloaded

Information for Authors: <http://jcp.aip.org/authors>

ADVERTISEMENT



AIPAdvances

Special Topic Section:
PHYSICS OF CANCER

Why cancer? Why physics? [View Articles Now](#)

Fluid-like behavior of a one-dimensional granular gas

Fabio Cecconi^{a)}

Dipartimento di Fisica, Università La Sapienza and INFM UdR Roma-1, P.le A. Moro 2, I-00185 Rome, Italy

Fabiana Diotallevi

Dipartimento di Fisica, Università La Sapienza, P.le A. Moro 2, I-00185 Rome, Italy

Umberto Marini Bettolo Marconi

Dipartimento di Fisica, Università di Camerino, Via Madonna delle Carceri, I-62032, Camerino, Italy and INFM, UdR Camerino, Italy

Andrea Puglisi

Dipartimento di Fisica, Università La Sapienza, P.le A. Moro 2, I-00185 Rome, Italy and INFM Center for Statistical Mechanics and Complexity, Rome, Italy

(Received 26 August 2003; accepted 10 October 2003)

We study the properties of a one-dimensional (1D) granular gas consisting of N hard rods on a line of length L (with periodic boundary conditions). The particles collide inelastically and are fluidized by a heat bath at temperature T_b and viscosity γ . The analysis is supported by molecular dynamics simulations. The average properties of the system are first discussed, focusing on the relations between granular temperature $T_g = m\langle v^2 \rangle$, kinetic pressure, and density $\rho = N/L$. Thereafter, we consider the fluctuations around the average behavior obtaining a slightly non-Gaussian behavior of the velocity distributions and a spatially correlated velocity field; the density field displays clustering: this is reflected in the structure factor which has a peak in the $k \sim 0$ region suggesting an analogy between inelastic hard core interactions and an effective attractive potential. Finally, we study the transport properties, showing the typical subdiffusive behavior of 1D stochastically driven systems, i.e., $\langle |x(t) - x(0)|^2 \rangle \sim Dt^{1/2}$, where D for the inelastic fluid is larger than the elastic case. This is directly related to the peak of the structure factor at small wave vectors. © 2004 American Institute of Physics. [DOI: 10.1063/1.1630957]

I. INTRODUCTION

Scientists and engineers have been studying granular materials for nearly two centuries for their relevance both in natural processes (landslides, dunes, Saturn rings) and in industry (handling of cereals and minerals, fabrication of pharmaceuticals, etc.).¹⁻⁴ The understanding of the “granular state” still represents an open challenge and one of the most active research topics in nonequilibrium statistical mechanics and fluid dynamics. For instance, a way to attack the problem consists of fluidizing the grains by shaking them so that the system behaves as a nonideal gas, a problem relatively easier to study. The difficulty, but also the beauty, of the dynamics of granular gases, meant as rarefied assemblies of macroscopic particles, stems from the inelastic nature of their collisions which leads to a variety of very peculiar phenomena. Several theoretical methods have been employed to deal with granular gases ranging from hydrodynamic equations, kinetic theories, to molecular dynamics. Engineers often prefer the strategy of the continuum description because it gives a better grasp of real-life phenomena, while natural scientists tend to opt for a microscopic approach to better control each step of the modelization. The latter, as far as the interaction between particles is concerned, regards granular systems as peculiar fluids, and treats them through the same

methods which have been successfully applied to ordinary fluids.⁵ This allows not only to employ concepts already developed by physicists and chemists, but also to stress analogies and substantial differences.

The purpose of the present paper is to establish such a connection for a system of stochastically driven inelastic hard rods constrained to move on a ring. The elastic version of this system has a long tradition⁶⁻¹² and is particularly suitable to test approximations and theories since many of its equilibrium properties can be derived in a closed analytical form. Even though the one-dimensional geometry introduces some peculiarities not shared by real fluids, we shall show that the model provides much useful information and a very rich phenomenology which closely recalls the behavior of microscopic particles confined in tubules or cylindrical pores with little interconnection. A second reason to investigate such a model is to show how the inelasticity of interactions influences not only the average global properties of a system, but also its microscopic local structure.

A basic requirement to a theoretical description of a granular gas is to provide an equation of state linking the relevant control parameters and possibly to relate it to the microscopic structure of the system. This connection is well known for classical fluids, where thermodynamic and transport properties are linked to the microscopic level via the correlation function formalism.

^{a)}Electronic mail: cecconif@roma1.infn.it

One-dimensional models have been employed by several authors as simple models of granular gases.^{13–24} The differences between the various models stem chiefly from the choice of the thermalizing device. In fact, granular gases would come to rest unless supplying energy compensating the losses due to the inelastic collisions. We call, by analogy, “heat bath” the external driving mechanism maintaining the system in a statistically steady state.

For the history, the first 1D models which were proposed had no periodic boundary conditions, and the energy was injected by a vibrating wall (stochastic or not). This kind of external driving, however, was not able to keep the system homogeneous, because only the first and last particle had a direct interaction with the wall.¹⁹ As an alternative, a uniform heating mechanism, namely a Gaussian white noise acting on each particle, was introduced.²⁰ Later, Puglisi *et al.*²¹ added a second ingredient, consisting of a friction term that prevents the kinetic energy from diverging. With such a modification the system reaches a steady regime and time averages can be safely computed. In the present paper we shall focus on this last model, characterizing its steady-state properties.

The layout is the following: In Sec. II we introduce the model, in Sec. III we obtain numerically and by approximate analytical arguments equations for the average kinetic energy and pressure. Section IV is devoted to fluctuations of the system observables around their average values. In Sec. V we study the diffusion properties of the system. Finally, in Sec. VI we present the conclusions.

II. THE MODEL

Inelastic hard sphere models are perhaps the simplest models able to capture the two salient features of granular fluids, namely the hard-core repulsion between grains and the dissipation of kinetic energy due to the inelastic collisions. Since many of the equilibrium properties of the 1D elastic hard rods are known in closed analytical form, such a system represents an excellent reference model even for the inelastic case. Let us consider N identical impenetrable rods, of coordinates $x_i(t)$, mass m , and size σ , constrained to move along a line of length L . Periodic boundary conditions are assumed. The hard-core character of the repulsive forces among particles reduces the interactions to single binary, instantaneous collision events occurring whenever two consecutive rods reach a distance $d_i(t) = x_i(t) - x_{i-1}(t)$ equal to their length σ . When two inelastic hard rods collide, their postcollisional velocities (primed symbols) are related to pre-collisional velocities (unprimed symbols) through the rule

$$v'_i = v_i - \frac{1+r}{2}(v_i - v_j), \quad (1)$$

where r indicates the coefficient of restitution. The interaction of each particle with the heat bath is represented by the combination of a viscous force proportional to the velocity and a stochastic force. Then each particle follows the so-called Kramers dynamics

$$\frac{dx_i}{dt} = v_i, \quad (2)$$

$$m \frac{dv_i}{dt} = -m\gamma v_i + \xi_i(t), \quad (3)$$

where γ is the viscous friction coefficient, $\xi_i(t)$ is a Gaussian white noise with zero average and correlation

$$\langle \xi_i(t) \xi_j(s) \rangle = 2\gamma m T_b \delta_{ij} \delta(t-s), \quad (4)$$

where T_b is the “heat-bath temperature” and $\langle \cdot \rangle$ indicates the average over a statistical ensemble of noise realizations.

We have developed a numerical simulation code for hard rods interacting through momentum-conserving but energy-dissipating collisions. In our simulations the motion between two consecutive collisions is governed by the dynamics (2) and (3). Thus, we determine the instant when the first collision among the N particles occurs and change its velocities and positions according to the equations of motion. The effect of the collision is taken into account by updating the velocities according to the rule (1).

We tested our code on the elastic case ($r=1$) and checked that our simulations faithfully reproduced the well-known properties of the equilibrium hard rod system.

III. AVERAGE PROPERTIES

We begin by considering the steady-state properties of the model. The aim is to derive relations connecting the microscopic parameters to the “thermodynamic” observables such as temperature and pressure, and eventually to obtain an “equation of state” relating these two quantities. In order to achieve this goal we assume that the system is homogeneous, so that its density ρ is constant.

A. Kinetic temperature

Collisions and the Kramers’ dynamics entail that the time derivative of the average kinetic energy per particle is

$$\frac{d}{dt} \frac{1}{2} m \langle v(t)^2 \rangle = \gamma(T_b - T_g) - w(t), \quad (5)$$

where $T_g = m \sum_{i=1}^N v_i^2 / N$ is the granular temperature and $w(t)$ is the average power dissipated by collisions, given by $w = [(1-r^2)/8] m \langle \delta v^2 \rangle / \tau_c$, where δv is the difference between the precollisional velocities of the colliding pair. The average collision time τ_c is estimated by assuming a mean free path $\lambda = (L - \sigma N) / N$, where $L - \sigma N$ is the free volume. We obtain, in terms of the system density $\rho = N/L$

$$\tau_c = \frac{\lambda}{v} = \frac{1 - \sigma\rho}{\rho} \sqrt{\frac{m}{T_g}}. \quad (6)$$

Thus, the average power dissipated per grain reads

$$w = \frac{1 - r^2}{8} \langle \delta v^2 \rangle \frac{\rho \sqrt{T_g m}}{1 - \sigma\rho}. \quad (7)$$

In order to estimate T_g we assume that $m \langle \delta v^2 \rangle \approx 4T_g$ since the velocities of the colliding pairs are strongly correlated. Thus, imposing the solution of Eq. (5) to be stationary we obtain for T_g the following expression:

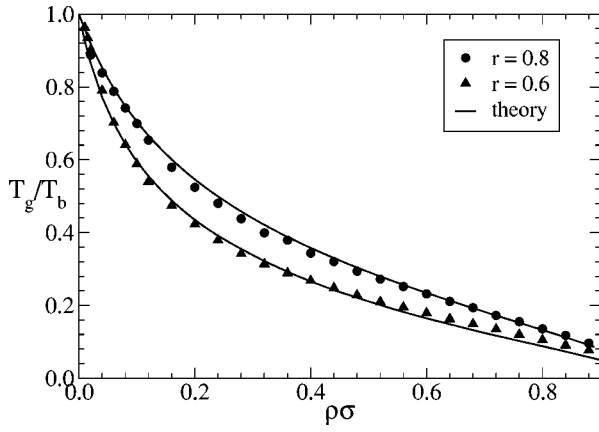


FIG. 1. Comparison between the numerical results for the granular temperature versus density and the corresponding theoretical expression, Eq. (8). The simulation data refer to $\sigma=0.2$, $\gamma=0.2$, $T_b=1.0$, $r=0.6$, and $r=0.8$. We kept the system size fixed to $L=40$ but varied the number of particles N to change the density.

$$T_g = \frac{T_b}{1 + \frac{1-r^2}{2\gamma} \frac{\rho}{1-\rho\sigma} \sqrt{\frac{T_g}{m}}} \quad (8)$$

In Fig. 1 we compare formula (8) with the results of numerical simulations at various densities. In spite of the simplicity of the argument used to derive Eq. (8), the agreement between T_g extracted by simulations and its theoretical estimate is fairly good.

B. Kinetic pressure

In a granular system the total pressure, P , can be obtained via its mechanical or kinetic definition, i.e., as the impulse transferred across a surface in the unit of time.^{25,26} The pressure contains both the ideal gas and the collisional contribution (P_{id} and P_{exc} , respectively)

$$P = P_{id} + P_{exc} = \rho T_g(\rho) + \frac{\sigma}{L t_{ob}} \sum_{k=1}^{M_c} \delta p_k, \quad (9)$$

where the second equality stems from the virial theorem.²⁷ Here, t_{ob} is the observation time, the sum runs over the M_c collisions, and $\delta p_k = m \delta v_k$ represents the impulse variation due to the k th collision.

An approximate formula for P_{exc} can be derived as follows. The average collision frequency per particle can be estimated as $\tau_c^{-1} = (M_c/t_{ob})/N$. By replacing in Eq. (9) t_{ob} with $(M_c/N)\tau_c$ and using τ_c given by Eq. (6), we obtain, for the excess part of the pressure, the expression

$$P_{exc} = \frac{N\sigma}{\tau_c L} m \langle \delta v_c \rangle = \frac{\rho^2 \sigma}{1 - \sigma \rho} T_g(\rho). \quad (10)$$

Collecting pieces together, we arrive at

$$P(\rho) = T_g(\rho) \left[\rho + \frac{\sigma \rho^2}{1 - \sigma \rho} \right] = T_g(\rho) \frac{\rho}{1 - \sigma \rho}, \quad (11)$$

which reproduces the well-known Tonks formula⁷ in the case of elastic particles and constitutes the equation of state

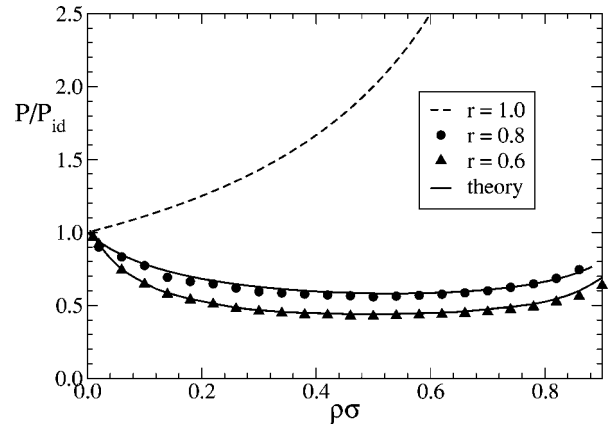


FIG. 2. Comparison between the kinetic pressure obtained from the simulations and the prediction of Eq. (11) at different densities for inelastic hard rods with coefficients of restitution $r=0.6$ and $r=0.8$. The dashed line refers to the pressure of the corresponding elastic system.

sought for the inelastic system. Let us recall that in the elastic case, Eq. (11) can be written in the virial form

$$P(\rho) = T_g(\rho) \rho [1 + \rho \sigma g(\sigma)], \quad (12)$$

showing the connection between the macroscopic and the microscopic level, since $g(\sigma) = 1/(1 - \rho\sigma)$ is the equilibrium pair correlation at contact.

We see from Fig. 2 that the presence of the prefactor $T_g(\rho)$, which is a decreasing function of the density, makes $P(\rho)$ increase more slowly than the corresponding pressure of the elastic system in the same physical conditions (i.e., same density and contact with the same heat bath).

Equations (8) and (10) for temperature and pressure coincide, in the limit $\gamma \rightarrow 0$, $\sigma \rightarrow 0$, $\gamma T_b = \Omega = \text{const}$, with those derived by Williams and MacKintosh.²⁰

Following the standard approach to fluids, we define, even for the inelastic system, the response of the density to a uniform change of the pressure for a fixed value of the heat-bath temperature

$$\chi_T = \frac{1}{\rho} \frac{\partial \rho}{\partial P}, \quad (13)$$

which is plotted in Fig. 3. We observe that the response of the inelastic system to a compression is much larger than the corresponding elastic system at the same density, due to the tendency to cluster.

IV. FLUCTUATIONS

So far, we have considered only the global average properties of the granular gas. It is well known, on the other hand, that these systems may exhibit strong spontaneous deviations from their uniform state. In this section we shall study fluctuations of the main observables in order to understand the qualitative effect of inelasticity on such a peculiar fluid.

A. Velocity distributions

One of the signatures of the inelasticity of the collisions is represented by the shape of the velocity distribution function (VDF), $P(v)$. Non-Gaussian VDFs, displaying low-velocity and high-velocity overpopulated regions, have

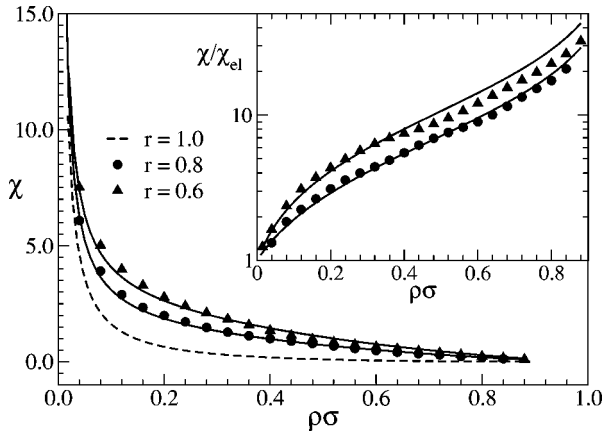


FIG. 3. Compressibility, computed from Eq. (13), plotted versus density, for inelastic hard rods with coefficient $r=0.6$ (the remaining parameters are the same as in Fig. 1). Symbols refers to simulations while solid lines are the theoretical predictions obtained via the expression for the pressure (11). The curve for the elastic system $r=1$ (dashed line) is also reported for sake of comparison. The inset shows the ratio between the inelastic and elastic compressibility.

been measured experimentally^{28–33} and in numerical simulations.^{21,34} In Fig. 4 we show two VDFs corresponding to two different values of r .

Theoretical, numerical, and experimental studies have shown that the VDF for inelastic ($r < 1$) gases usually displays overpopulated tails. The literature seems to indicate the lack of a universal VDF: in $d > 1$ the solution of the homogeneous Boltzmann equation with inelastic collisions (with a stochastic driving similar to ours but without viscosity) has overpopulated tails of the kind $\sim \exp(-v^{3/2})$.³⁵

B. Energy fluctuations

Interestingly, the energy fluctuations of our system, $E \equiv m \sum_i v_i^2 / 2$, display a scaling with respect to the number of particles. We are interested in the quantity $(\langle E^2 \rangle - \langle E \rangle^2) / \langle E \rangle^2$ as a function of N (at fixed density ρ). Defining $\langle v^n \rangle = \int v^n P(v) dv$, we have

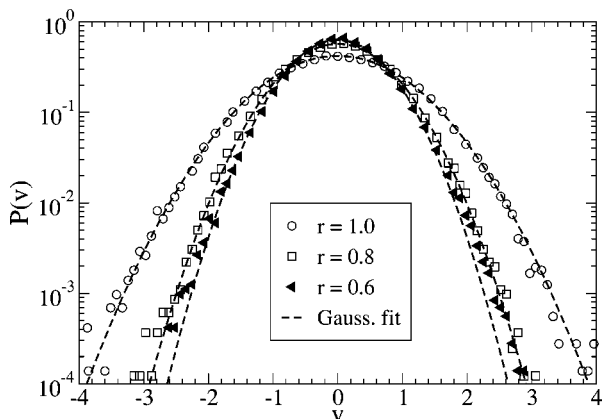


FIG. 4. Velocity distributions $P(v)$ for three values of the coefficient of restitution $r=1.0$ (circles), 0.8 (squares), 0.6 (triangles). The remaining parameters are $N=1000$, $L=1000$, $\sigma=0.2$, $T_b=1.0$, $\gamma=0.2$. Dashed lines indicate the corresponding Gaussian fit.

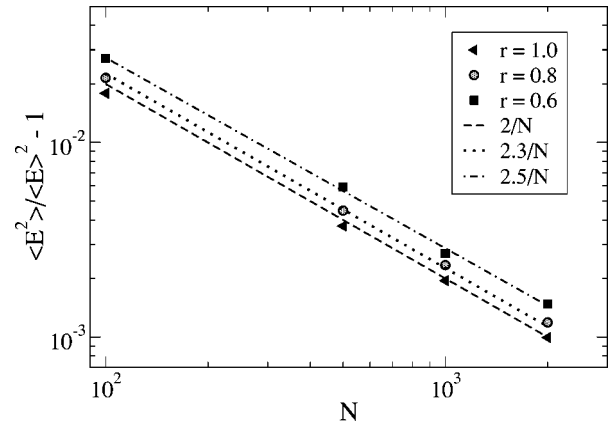


FIG. 5. Energy fluctuation as a function of the number of particles, N for $r=1.0, 0.8, 0.6$. The elastic case agrees with the theoretical prediction $2/N$, whereas the inelastic case gives a value of the relative fluctuation slightly larger. The remaining parameters are the same as in Fig. 4.

$$\langle E^2 \rangle - \langle E \rangle^2 = \frac{m^2}{4} \sum_{i,j} (\langle v_i^2 v_j^2 \rangle - \langle v_i^2 \rangle \langle v_j^2 \rangle). \quad (14)$$

Under the hypothesis that the variables v_i are independently distributed, we get

$$\langle E^2 \rangle - \langle E \rangle^2 = \frac{m^2}{4} [N \langle v^4 \rangle - N \langle v^2 \rangle^2]. \quad (15)$$

Since for Gaussian variables $\langle v^4 \rangle = 3 \langle v^2 \rangle^2$, we find

$$\frac{\langle E^2 \rangle - \langle E \rangle^2}{\langle E \rangle^2} = \frac{2}{N}, \quad (16)$$

which is a well-known formula for equilibrium systems.³⁶ This scaling is fairly well verified in Fig. 5.

In the case of a granular fluid, $P(v_i)$ is no longer Gaussian, exhibiting fatter tails, so one observes $\langle v^4 \rangle \geq 3 \langle v^2 \rangle^2$ (for example, in the case $r=0.6$ we have $\langle v^4 \rangle / \langle v^2 \rangle^2 \approx 3.3$). This leads to the conclusion that the scaling $\sim 1/N$ of formula (16) still holds, but with a coefficient larger than 2. Simulation runs for $r=0.6$ confirm this prediction (Fig. 5). The renormalization of the multiplicative constant occurring in the inelastic system could be interpreted also as an “effective reduction” of the number of degrees of freedom. Indeed, the inelastic system has the tendency to cluster, as it will be shown, and therefore the effective number of independent “particles” appears smaller. Another appealing interpretation is that the inelastic systems possesses an effective “specific heat” larger than that of elastic systems.

C. Velocity correlations

A universal signature of the inelasticity is the presence of correlations between the velocities of the particles. We measured the structure function of the velocities v_i , $S_v(k) = \langle \tilde{v}(k) \tilde{v}(-k) \rangle$, where $\tilde{v}(k)$ is the Fourier transform of v_i . In Fig. 6, we show three $S_v(k)$ corresponding to the elastic ($r=1$) and inelastic system with $r=0.8$ and $r=0.6$. As mentioned above, the elastic system is characterized by uncorrelated velocities, and this reflects on a constant structure function. A certain degree of correlation is instead evident in the

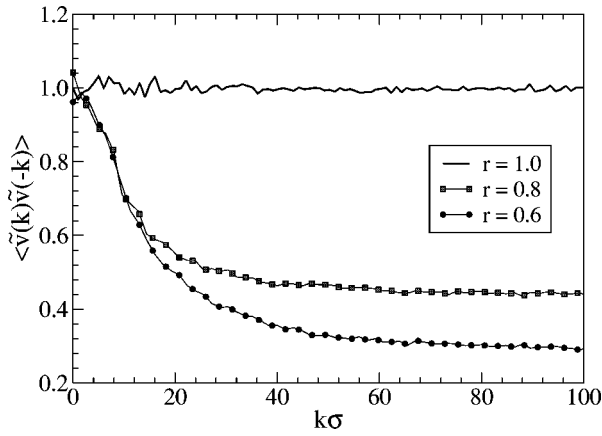


FIG. 6. Structure function of the velocity field v_i , for elastic and inelastic systems. The control parameters are the same as in Fig. 4.

inelastic system. In fact, the inelasticity reduces by a factor r the relative velocity of two colliding particles, and this leads to an increasing correlation among velocities. However, the noise induced by the bath competes with these correlations, making the structure function not very steep. More specifically, $S_v(k)$ can be fitted, in the middle range of k values, by an inverse power $\sim k^{-0.5}$, while at high k values it reaches a constant plateau. This is the fingerprint of a persistent internal noise (velocity fluctuations are not completely frozen by inelastic collisions).³⁷

D. Distribution of interparticle spacing and of collision times

The probability distribution, $P(\delta x)$, of distances between nearest-neighbor particles $\delta x = x_i - x_{i-1}$, shown in Fig. 7, provides information about the spatial arrangement of the system. In the elastic case, one easily finds

$$P(\delta x) = \frac{1}{\lambda} \exp[-(\delta x - \sigma)/\lambda], \quad (17)$$

for $\delta x \geq \sigma$ and 0 for $\delta x < \sigma$ with $\lambda = (1 - \rho\sigma)/\rho$. The presence of inelasticity modifies such a simple exponential law in

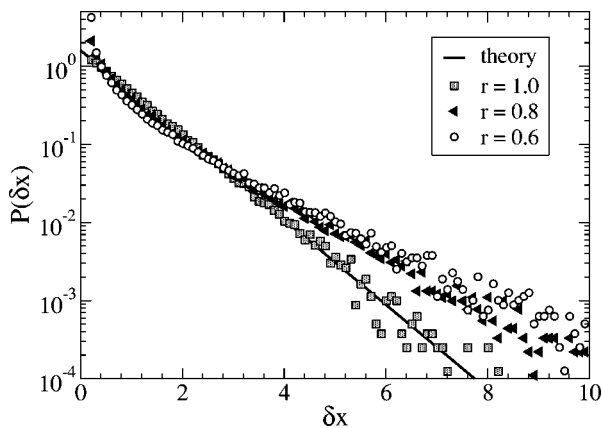


FIG. 7. Distributions of distances between nearest-neighbor particles $\delta x = x_i - x_{i-1}$, for elastic and inelastic systems, with the same parameters used before. The solid line indicates the exponential expected in the elastic case (see the text). The state parameters are the same as in Fig. 4.

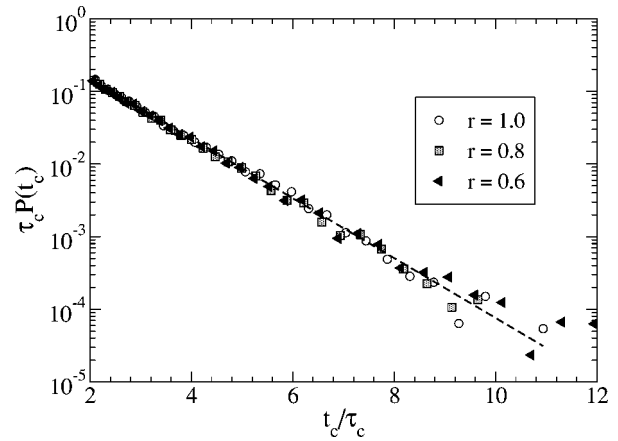


FIG. 8. Distributions of collision times. The dashed line indicates the exponential law expected for the elastic system (see the text). Control parameters as in Fig. 7.

the way shown in Fig. 7. In this case, the probability of finding two particles at small separation increases together with that of finding large voids. Such a picture is consistent with the idea of the clustering phenomenon:³⁸ Two particles, after the inelastic collision, have a smaller relative velocity and therefore reach smaller distances, eventually producing dense clusters and leaving larger empty regions with respect to the elastic case.

On the contrary, the probability distribution of collision times, shown in Fig. 8, appears to always follow the theoretical (elastic) form $P(t) = 1/\tau_c \exp(-t/\tau_c)$. Apart from a trivial rescaling due to the change of the thermal velocity with r , it seems not to depend appreciably on the coefficient of restitution.

Such a finding is in contrast with the situation observed in 2D vibrated granular systems.^{30,39} A possible explanation for this discrepancy is the following: In the inelastic 1D system, there is a correlation between the relative velocities and the free paths (or free times); otherwise, the distribution $P(t)$ and $P(\delta x)$ would have had the same shape due to the trivial relation $x = vt$, v being the the average velocity of the rods. In particular, the fact that the peak of $P(\delta x)$ in $\delta x = 0$ does not yield a corresponding peak in the $t = 0$ region of $P(t)$ suggests that the shorter the distance between particles the smaller their relative velocity.

E. Density fluctuations

We turn now to the study of the structural properties of the inelastic hard rod gas, by considering the pair correlation function or the structure factor. As mentioned in Sec. II, the virial equation (12) relates the pressure of an elastic hard rod system to its microscopic structure. In the presence of inelasticity, however, we expect that the tendency to cluster is mirrored by a change in the structural properties of the fluid. Therefore, we considered the behavior of the static (truly speaking steady state) structure factor

$$S(k) = 1 + \rho \int dx [g(x) - 1] e^{ikx}, \quad (18)$$

for different values of $\rho\sigma$ and inelasticity.

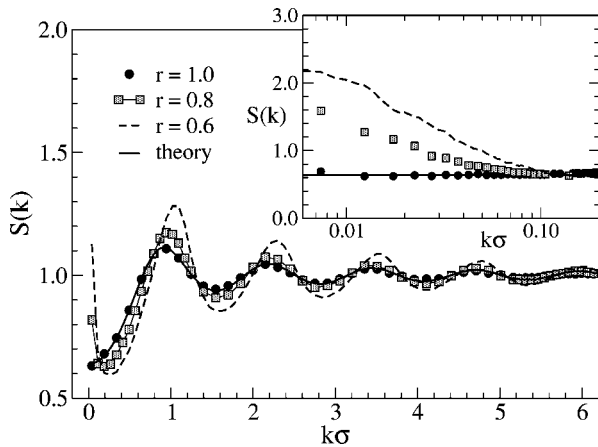


FIG. 9. Typical behavior of the structure function of $S(k)$ for different values of the coefficients $r=1.0, 0.8, 0.6$. Notice the growth of the peak at small k when r decreases.

The spatial structure of the system is determined, as in ordinary fluids, by the strong repulsive forces. Their role is seen in the oscillating structure of $g(x)$. The inelastic nature of the collisions provides a correction to $g(x)$, which can be better appreciated by studying the small wavelength behavior of $S(k)$ which develops a peak at small k recalling the Ornstein–Zernike behavior

$$S(k) \approx \frac{1}{S^{-1}(0) + c_2 k^2}. \quad (19)$$

The coefficient c_2 is negative for hard rods, whereas it is positive for the inelastic system. For hard rods, $S(k)$ is known¹² and reads

$$S(k) = \frac{1}{1 + 2b\rho\sigma \frac{\sin(k\sigma)}{k\sigma} + (b\rho\sigma)^2 \frac{\sin^2(k\sigma/2)}{(k\sigma/2)^2}}, \quad (20)$$

with $b = 1/(1 - \rho\sigma)$.

Figure 9 shows the typical behaviors of $S(k)$ for elastic and inelastic systems. The numerically computed structure factor of the elastic system agrees rather well with Eq. (20). The inelastic system, instead, displays a peak in the small k region, reflecting the tendency of the fluid to cluster. The peak increases with inelasticity, demonstrating that the energy dissipation in collisions is responsible for these long-range correlations. Incidentally, we comment that such a behavior of $S(k)$ could be attributed to the presence of a long-range attractive effective potential between the rods, as a result of dynamical correlations.⁴⁰

Mackintosh and Williams²⁰ found that, in the case of randomly kicked rods in the absence of viscosity, the pair correlation function decays as an inverse power law, $g(x) \propto x^{-\eta}$, with $\eta \rightarrow 0$ for $r \rightarrow 1$ and $\eta \rightarrow 1/2$ for $r \rightarrow 0$. Correspondingly, one expects $S(k)$ to diverge as $k^{-1/2}$ as $k \rightarrow 0$, for very inelastic systems. In other words, the inelasticity leads to long-range spatial correlations which are revealed by the peak at small k of $S(k)$. We remark that, in spite of the apparent similarity between the equations of state for elastic and inelastic systems, their structural properties are radically different. Such a phenomenon is the result of the coupling of

the long-wavelength modes of the velocity field with the stochastic nonconserved driving force. In fact, due to the inelastic collisions, the velocities of the particles tend to align, thus reducing the energy dissipation. On the other hand, these modes adsorb energy from the heat bath and grow in amplitude, and only the presence of friction prevents these excitations from becoming unstable. The density field, which is coupled to the velocity field by the continuity equation, also develops long-range correlations, and the structure factor displays a peak at small wave vectors.

V. TRANSPORT PROPERTIES

One-dimensional hard-core fluids exhibit an interesting connection between the microscopic structural properties and diffusive ones. In the present section, we present numerical results for the collective diffusion and for the diffusion of a tagged particle, and show how these are connected to the structure.

A. Collective diffusion and self-diffusion

Let us turn to analyze the perhaps simplest transport property of the hard rods system, namely the self-diffusion, i.e., the dynamics of a grain in the presence of $N-1$ partners. The problem is highly nontrivial since the single grain degrees of freedom are coupled to those of the remaining grains. Such a single-filing diffusion is also relevant in the study of transport of particles in narrow pores.⁴¹

The diffusing particles can never pass each other. The excluded volume effect represents a severe hindrance for the particles to diffuse. In fact, a given particle in order to move must wait for a collective rearrangement of the entire system. Only when the cage of a particle expands is the tagged particle free to diffuse further. This is a peculiar form of the so-called cage effect, which is enhanced by the one-dimensional geometry. In addition, the cage effect produces a negative region and a slow tail in the velocity autocorrelation function.

As an appropriate measure of the self-diffusion, we consider the average square displacement of each particle from its position at a certain time, that we assume to be $t=0$ without loss of generality

$$R(t) = \frac{\sum_{i=1}^N \langle [x_i(t) - x_i(0)]^2 \rangle}{N}. \quad (21)$$

At an early stage, the self-diffusion is expected to display ballistic behavior, $R(t) \sim |v|^2 t^2$, with $|v|^2 = T_g/m$, before any perturbation (heat bath and collisions) change the free motion of particles, i.e., when $t \ll 1/\gamma$ and $t \ll \tau_c$.

A system of noninteracting (i.e., noncolliding) particles subjected to Kramers' dynamics (2), (3) displays, after the ballistic transient, normal self-diffusion of the form $R(t) \sim 2D_0 t$ with $D_0 = T_g/\gamma$. This is well verified in Fig. 10 (circles).

Lebowitz and Percus⁴² studied the tagged particle diffusion problem for systems governed by nondissipative dynamics without heat bath and found a diffusive behavior described by

$$R(t) = 2D_{\text{coll}} t = \lambda \langle |v| \rangle t, \quad (22)$$

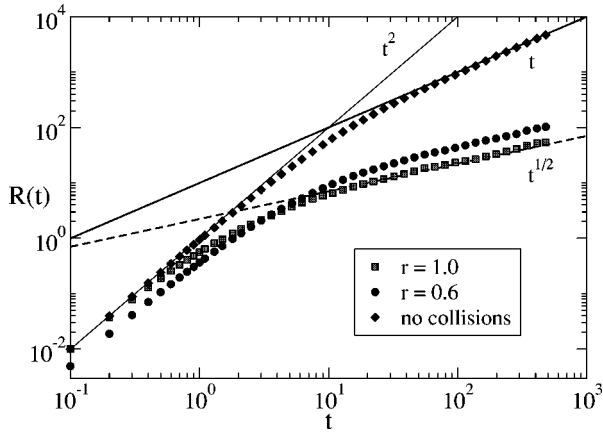


FIG. 10. Self-diffusion: Behavior of $R(t)$ for three different systems: one without collisions (free particles), one with elastic collisions, and the third with inelastic collisions ($r=0.6$).

with $\lambda = (1 - \rho\sigma)/\rho$. Since $\langle |v| \rangle = \sqrt{T/2\pi m}$, one obtains

$$D_{\text{coll}} = \frac{1 - \rho\sigma}{\rho} \sqrt{\frac{T}{2\pi m}}. \quad (23)$$

On the other hand, almost in the same years, Harris⁴³ studied the behavior of $R(t)$ in the case of N identical Brownian particles with hard-core interactions, i.e., obeying a single-filing condition, and obtained a subdiffusive behavior increasing as

$$R(t) = 2\lambda \left(\frac{D_0 t}{\pi} \right)^{1/2}, \quad (24)$$

where D_0 is the single (noninteracting) particle diffusion coefficient.

In Fig. 10, we plot the self-diffusion $R(t)$ for elastic and inelastic systems in the presence of heat bath and viscosity, obtaining two different regimes separated by a typical time τ_c . In the first transient regime $t < \tau_c$ we observe the ballistic motion. In the second stage, instead, we expect the subdiffusive behavior, $R(t) \sim t^{1/2}$, predicted by Harris and other authors.⁴³⁻⁴⁵ The inelastic system displays the same subdiffusive behavior, but with a multiplicative constant larger than 1, i.e., at equal times the granular (inelastic) fluid has a larger absolute value of $R(t)$.

It is interesting to analyze the connection between this transport property and the compressibility of the system, as remarked by Kollmann.⁴¹

B. Connection between self-diffusion and structure

We follow Alexander and Pincus' argument⁴⁴ in order to derive a formula for the self-diffusion and show the connection with the compressibility of the system. Let us consider the two-time correlator

$$\langle \rho_k(t) \rho_{-k}(0) \rangle = \sum_{ij} \langle e^{ikx_i(t)} e^{-ikx_j(0)} \rangle. \quad (25)$$

We set $x_i(t) = X_i + (x_i(t) - X_i) = X_i + u_i$, where X_i are the nodes of the 1D lattice $X_i = ia$ (a being the lattice spacing). Expanding around X_i

$$\langle \rho_k(t) \rho_{-k}(0) \rangle \approx k^2 \sum_{ij} e^{ik(X_i - X_j)} \langle u_i(0) u_j(t) \rangle; \quad (26)$$

hence

$$\langle \hat{u}_k(t) \hat{u}_{-k}(0) \rangle = \frac{\langle \rho_k(t) \rho_{-k}(0) \rangle}{Nk^2}. \quad (27)$$

We assume now that the density correlator varies as

$$\langle \rho_k(t) \rho_{-k}(0) \rangle = \langle \rho_k(0) \rho_{-k}(0) \rangle e^{-Dk^2 t}, \quad (28)$$

where $D = D_0/S(0)$ (this is demonstrated in the Appendix) is the collective diffusion coefficient, with $D_0 = T_b/\gamma$. Now, the mean square displacement per particle (21) can be written as $R(t) = \sum_j \langle [u_j(t) - u_j(0)]^2 \rangle / N$ and, in Fourier components, reads

$$R(t) = \frac{2}{N} \sum_k \langle \hat{u}_k(0) \hat{u}_{-k}(0) - \hat{u}_k(t) \hat{u}_{-k}(0) \rangle. \quad (29)$$

Employing Eq. (27), we find

$$R(t) = 2 \sum_k \langle \rho_k(0) \rho_{-k}(0) \rangle \frac{1 - e^{-Dk^2 t}}{N^2 k^2}. \quad (30)$$

Approximating the sum with an integral, $\sum_k \rightarrow L/(2\pi) \int_{-\pi/a}^{\pi/a} dk$, and recalling that

$$NS(k) = \langle \rho_k(0) \rho_{-k}(0) \rangle, \quad (31)$$

we obtain

$$R(t) = \frac{2L}{N} \int_0^{\pi/a} \frac{dk}{2\pi} S(k) \frac{1 - e^{-Dk^2 t}}{k^2}, \quad (32)$$

and therefore

$$R(t) \approx \frac{2}{\rho\pi} S(0) \sqrt{\pi D t} = \frac{2}{\rho} \sqrt{\frac{D_0 S(0) t}{\pi}}. \quad (33)$$

Notice that such a formula in the case of hard rods is identical to formula (24).

We see that the tagged particle diffusion depends on the structure of the fluid. In the granular fluid the $k \rightarrow 0$ part of the spectrum is enhanced and thus we expect a stronger tagged particle diffusion. This is what we observe. Physically there are larger voids and particles can move more freely. Let us notice that as far as the collective diffusion is involved the spread of a group of particles is faster in the presence of repulsive interactions than without.⁴⁶

VI. CONCLUSIONS

In this paper we have studied a one-dimensional system of inelastic hard rods coupled to a stochastic heat bath with the idea that it can represent a reference system in the area of granular gases to test theories and approximations. Due to the relative simplicity of the one-dimensional geometry, we have shown that it is possible to obtain relations between the macroscopic control parameters such as kinetic temperature, pressure, and density. We tested these analytical predictions against the numerical measurements and found a fairly good agreement. It also appears that many properties of the heated one-dimensional inelastic hard rod system are similar to

those of ordinary fluids. However, when we have considered how various physical observables fluctuate about their equilibrium values, many relevant differences have emerged. These range from the non-Gaussian behavior of the velocity distribution, the peculiar form of the distribution of distances between particles and of the energy fluctuations, to the shape of the structure factor at small wave vectors. Finally, we have found that the diffusive properties of the system are affected by the inelasticity and, in particular, the self-diffusion is enhanced.

To conclude, in spite of the similarity between ordinary fluids and granular fluids, which has been recognized for many years and has made it possible to formulate hydrodynamical equations for granular media in rapid, dilute flow, the presence of anomalous fluctuations in the inelastic case indicates the necessity of a treatment which incorporates in a proper way both the local effects such as the excluded volume constraint and the long-ranged velocity and density correlations. Such a program has been partially carried out by Ernst and co-workers,³⁷ but needs to be completed regarding the description of the fluid structure.

APPENDIX: COLLECTIVE DIFFUSION COEFFICIENT

In the case of overdamped dynamics (i.e., large values of γ) one finds that the collective diffusion is given by⁴⁶

$$\frac{\partial \rho(x,t)}{\partial t} = \frac{1}{\gamma} \frac{\partial}{\partial x} \left\{ \rho(x,t) \frac{\partial \mu(\rho(x))}{\partial x} \right\}, \quad (\text{A1})$$

where $\mu(\rho(x))$ is the local chemical potential. Expanding μ about its average value ρ_0 , we obtain

$$\frac{\partial \mu(\rho(x))}{\partial x} = \left[\frac{\delta \mu}{\delta \rho} \right]_{\rho_0} \frac{\partial \rho(x)}{\partial x}. \quad (\text{A2})$$

Substituting into Eq. (A1), we find

$$\frac{\partial \rho(x,t)}{\partial t} = \frac{1}{\gamma} \rho_0 \left[\frac{\delta \mu}{\delta \rho} \right]_{\rho_0} \frac{\partial^2 \rho(x)}{\partial x^2}, \quad (\text{A3})$$

and using

$$S(0) = \frac{K_B T_b}{\rho_0} \left[\frac{\partial \rho_0}{\partial \mu} \right]_T \quad (\text{A4})$$

in the case of elastic hard rods, we obtain

$$\frac{\partial \rho(x,t)}{\partial t} = \frac{1}{\gamma} \frac{K_B T_b}{S(0)} \frac{\partial^2 \rho(x)}{\partial x^2} = \frac{D_0}{S(0)} \frac{\partial^2 \rho(x)}{\partial x^2}. \quad (\text{A5})$$

Thus, the renormalized diffusion coefficient is $D = D_0/S(0)$.

¹H. M. Jaeger, S. R. Nagel, and R. P. Behringer, *Rev. Mod. Phys.* **68**, 1259 (1996) and references therein.

- ²J. Duran, *Sands, Powders and Grains: An Introduction to the Physics of Granular Materials* (Springer, New York, 2000).
- ³L. P. Kadanoff, *Rev. Mod. Phys.* **71**, 435 (1999).
- ⁴*Granular Gases*, Lectures Notes in Physics Vol. **564**, edited by T. Pöschel and S. Luding (Springer, Berlin Heidelberg, 2001).
- ⁵J. P. Hansen and I. R. MacDonald, *Theory of Simple Liquids* (Academic, London, 1990).
- ⁶Lord Rayleigh, *Nature (London)* **45**, 80 (1995).
- ⁷L. Tonks, *Phys. Rev.* **50**, 955 (1936).
- ⁸H. Takahashi, *Proc. Phys. Math. Soc. Jpn.* **24**, 60 (1942).
- ⁹J. Frenkel, *Kinetic Theory of Liquids* (Oxford University Press, New York, 1940).
- ¹⁰F. Gurse, *Proc. Cambridge Philos. Soc.* **46**, 182 (1950).
- ¹¹Z. Salsburg, R. Zwanzig, and J. Kirkwood, *J. Chem. Phys.* **21**, 1098 (1953).
- ¹²J. K. Percus, *J. Stat. Phys.* **15**, 505 (1976).
- ¹³J. M. Pasini and P. Cordero, *Phys. Rev. E* **63**, 041302 (2001).
- ¹⁴N. Sela and I. Goldhirsch, *Phys. Fluids* **7**, 507 (1995).
- ¹⁵S. McNamara and W. R. Young, *Phys. Fluids A* **4**, 496 (1992); **5**, 34 (1993).
- ¹⁶E. L. Grossman and B. Roman, *Phys. Fluids* **8**, 3218 (1996).
- ¹⁷T. Zhou, *Phys. Rev. Lett.* **80**, 3755 (1998).
- ¹⁸T. Zhou, *Phys. Rev. E* **58**, 7587 (1998).
- ¹⁹Y. Du, H. Li, and L. P. Kadanoff, *Phys. Rev. Lett.* **74**, 1268 (1995).
- ²⁰D. R. M. Williams and F. C. MacKintosh, *Phys. Rev. E* **54**, R9 (1996).
- ²¹A. Puglisi, V. Loreto, U. M. B. Marconi, A. Petri, and A. Vulpiani, *Phys. Rev. Lett.* **81**, 3848 (1998); *Phys. Rev. E* **59**, 5582 (1999).
- ²²F. Cecconi, A. Puglisi, U. M. B. Marconi, and A. Vulpiani, *Phys. Rev. Lett.* **90**, 064301 (2003).
- ²³E. Ben-Naim, S. Y. Chent, G. D. Doolent, and S. Redner, *Phys. Rev. Lett.* **83**, 4069 (1999).
- ²⁴A. Baldassarri, U. Marini Bettolo Marconi, and A. Puglisi, *Europhys. Lett.* **58**, 14 (2002).
- ²⁵M. P. Allen and D. J. Tildesley, *Computer Simulation of Liquids* (Clarendon, Oxford, 1987).
- ²⁶A. Barrat and E. Trizac, *Phys. Rev. E* **66**, 051303 (2002).
- ²⁷J. J. Erpenbeck and W. W. Wood, *Statistical Mechanics B. Modern Theoretical Chemistry*, edited by J. Berne (Plenum, New York, 1977), Vol. 6.
- ²⁸W. Losert, D. G. W. Cooper, J. Delour, A. Kudrolli, and J. P. Gollub, *Chaos* **9**, 682 (1999).
- ²⁹K. Feitosa and N. Menon, *Phys. Rev. Lett.* **88**, 198301 (2002).
- ³⁰D. L. Blair and A. Kudrolli, *Phys. Rev. E* **67**, 041301 (2003).
- ³¹J. S. Olafsen and J. S. Urbach, *Phys. Rev. Lett.* **81**, 4369 (1998).
- ³²I. S. Aranson and J. S. Olafsen, *Phys. Rev. E* **66**, 061302 (2002).
- ³³A. Kudrolli and J. Henry, *Phys. Rev. E* **62**, R1489 (2000).
- ³⁴J. J. Brey and M. J. Ruiz-Montero, *Phys. Rev. E* **67**, 021307 (2003).
- ³⁵T. P. C. van Noije and M. H. Ernst, *Granular Matter* **1**, 57 (1998).
- ³⁶K. Huang, *Statistical Mechanics* (Wiley, New York, 1987).
- ³⁷T. P. C. van Noije, M. H. Ernst, E. Trizac, and I. Pagonabarraga, *Phys. Rev. E* **59**, 4326 (1999).
- ³⁸I. Goldhirsch and G. Zanetti, *Phys. Rev. Lett.* **70**, 1619 (1993).
- ³⁹D. Paolotti, C. Cattuto, U. Marini Bettolo Marconi, and A. Puglisi, *Granular Matter* **5**, 75 (2003).
- ⁴⁰T. P. C. van Noije, M. H. Ernst, R. Brito, and J. A. G. Orza, *Phys. Rev. Lett.* **79**, 411 (1997).
- ⁴¹M. Kollmann, *Phys. Rev. Lett.* **90**, 180602 (2003).
- ⁴²J. L. Lebowitz and J. K. Percus, *Phys. Rev.* **155**, 122 (1967).
- ⁴³T. E. Harris, *J. Appl. Probab.* **2**, 323 (1965).
- ⁴⁴S. Alexander and P. Pincus, *Phys. Rev. B* **18**, 2011 (1978).
- ⁴⁵H. van Beijeren, K. W. Kehr, and R. Kutner, *Phys. Rev. B* **28**, 5711 (1983).
- ⁴⁶U. Marini Bettolo Marconi and P. Tarazona, *J. Chem. Phys.* **110**, 8032 (1999); *J. Phys.: Condens. Matter* **12**, A413 (2000).